ResearchGate

See discussions, stats, and author profiles for this publication at: https://www.researchgate.net/publication/244328717

Evidence of coupled photoinduced proton transfer and intramolecular charge transfer reaction in para-N,N-dimethylamino orthohydroxy benzaldehyde: Spectroscopic and theoretical stud...

ARTICLE *in* CHEMICAL PHYSICS · DECEMBER 2008

Impact Factor: 1.65 · DOI: 10.1016/j.chemphys.2008.10.002

CITATIONS
16

READS
35

4 AUTHORS, INCLUDING:

Subrata Mahanta
National Institute of Advanced Industrial Sc...
25 PUBLICATIONS **398** CITATIONS
SEE PROFILE

Rupashree Balia Singh
National Institute of Advanced Industrial Sc...
27 PUBLICATIONS **419** CITATIONS
SEE PROFILE

Available from: Subrata Mahanta
Retrieved on: 24 January 2016

Chemical Physics 354 (2008) 118–129

Contents lists available at ScienceDirect

Chemical Physics

journal homepage: www.elsevier.com/locate/chemphys

Evidence of coupled photoinduced proton transfer and intramolecular charge transfer reaction in para-N,N-dimethylamino orthohydroxy benzaldehyde: Spectroscopic and theoretical studies

Subrata Mahanta, Rupashree Balia Singh, Samiran Kar [1], Nikhil Guchhait *

Department of Chemistry, University of Calcutta, 92, A.P.C. Road, Kolkata 700009, India

ARTICLE INFO

Article history:
Received 2 May 2008
Accepted 8 October 2008
Available online 11 October 2008

Keywords:
Para-N,N-dimethylamino orthohydroxy benzaldehyde (PDOHBA)
Proton transfer
Charge transfer
Hartree Fock (HF)
Density Functional Theory (DFT)

ABSTRACT

Steady state and time resolved fluorescence spectroscopy and quantum chemical calculations have been used to study excited state properties of para-N,N-dimethylamino orthohydroxy benzaldehyde (PDOHBA). Spectral characteristics of PDOHBA support the existence of both donor–acceptor charge transfer (CT) and proton transfer (PT) reaction in the excited state. Structural calculations at Hartree Fock and Density Functional Theory (DFT) levels and theoretical potential energy surfaces (PESs) along the proton transfer and donor twisting coordinates using DFT and Time Dependent Density Functional Theory point towards the possibility of barrierless PT and CT reaction in the first excited state of PDOHBA.
© 2008 Elsevier B.V. All rights reserved.

1. Introduction

The excited state intramolecular proton transfer (ESIPT) and intramolecular charge transfer (CT) reactions are the most important photoinduced phenomena studied by several groups due to their wide applications in the basic and applied research [1–30]. Since the first observation of dual fluorescence in methyl salicylate (MS) by Weller in 1956 [1], a variety of molecular systems have been studied experimentally and theoretically for the possibility of ESIPT reaction [1–20]. Significant interest rests on the fundamental investigation and the application of organic molecules exhibiting ESIPT reaction because of their four-level photophysical process, and a large Stokes shifted characteristics fluorescence emission band. The ESIPT process is a photo-tautomerization process, i.e., enol (E) to keto (K) transformation in the excited state via an intramolecular hydrogen bond involving the transfer of hydroxyl proton to the electronegative atom, which occurs extremely fast in the subpicosecond time scale [9]. After the relaxation of the keto form to the ground state, the energetically favored enol form is recovered spontaneously by reverse proton transfer to complete the cyclic four-level scheme. Consequently, this process gives rise to the transient chemical change from enol to keto tautomer, leading to the transient alternation of the electronic properties such as electron density distribution, energies of electronic states, and dipole moment etc. Recently, it has been demonstrated that proper structural design of ESIPT molecules provide peculiar and interesting properties such as electrochromic modulation, anion emission, perturbation of electronic state by variation of solvent polarity. Molecules giving rise to excited state tautomer by intramolecular proton transfer are often used as laser dyes, molecular memory storage devices, fluorescent probes and polymer protectors [31–34].

Side by side the excited state intramolecular charge transfer (ICT) process has received a great attention since the first observation of dual fluorescence from para-N,N-dimethyl amino benzonitrile (DMABN) in polar solvents by Lippert et al. [21]. In polar solvents, DMABN shows a large Stokes shifted emission band apart from the normal emission from the locally excited (LE) state. Many experimental and theoretical studies have been performed on DMABN and related donor–acceptor charge transfer systems to establish the mechanism of excited state ICT process [21–30]. So far, models such as twisted intramolecular charge transfer (TICT) [22–24,26–29], planarized intramolecular charge transfer (PICT) [25], wagging intramolecular charge transfer (WICT) [30] have been proposed to establish ICT reaction in different donor–acceptor charge transfer molecular systems. According to the most accepted TICT model donor and acceptor, perpendicular geometry

* Corresponding author. Tel.: +91 33 250 8386; fax: +91 33 2351 9755.
E-mail addresses: nguchhait@yahoo.com, nikhil.guchhait@rediffmail.com (N. Guchhait).
[1] Present address: CHEMGEN Pharma International, Dr. Siemens Street, Block GP, Sect. V, Salt Lake City, Kolkata 700091, India.

0301-0104/$ - see front matter © 2008 Elsevier B.V. All rights reserved.
doi:10.1016/j.chemphys.2008.10.002

generates a decoupled state leading to the formation of a CT state which is stabilized by polar solvents and is responsible for solvent polarity dependent red-shifted emission [22–24]. Similar to molecules having ESIPT capability, the donor–acceptor ICT molecules are interesting due to their vast applications in the field of pure and applied sciences such as nonlinear optical and electro-optical materials, pH and ion detectors, fluorescence sensors, etc. [35–42]. The photo induced intramolecular charge transfer (ICT) reaction may also play a crucial role in vision [43] and in biological light harvesting processes such as photosynthesis [44].

Molecules of diverse complexities have been studied but the most important and interesting ones are those with bifunctional groups having both the proton donor–acceptor and the charge donor–acceptor abilities within the same system. In most cases, the PT and the ICT reactions are considered to be decoupled as was observed in ultrafast pump-probe experiments [45]. The competition between excited state CT and PT processes have been studied systematically by Kasha's group in some molecular systems [46]. They observed both CT and PT processes in p-dimethylaminosalicylic acid methyl ester (DMASAME) having donor–acceptor charge transfer site and intramolecular hydrogen bonded proton translocation site. Usually such types of systems tend to exhibit stronger acidity and basicity in the excited state leading to transfer of proton from acidic to basic moiety and also have charge transfer ability from donor to the acceptor group upon excitation. Very recently, Chou's group and Rodriguez-Prieto's group reported coupled PT and CT reaction in some interesting molecular systems [47–49]. In this work, we present photoinduced process in PDOHBA having donor and acceptor moiety suitable for excited state ICT reaction as well as the presence of six member IMHB ring capable for ESIPT reaction. The molecule PDOHBA consists of two basic units, one is the orthohydroxybenzaldehyde (OHBA) unit capable for ESIPT process [50–56] and the other is the 4-dimethylaminobenzaldehyde (DMABA) suitable for ICT reaction [57–58]. In PDOHBA, comparatively weak charge acceptor aldehyde group is present instead of strong charge acceptor ester group in DMASAME molecule. Our

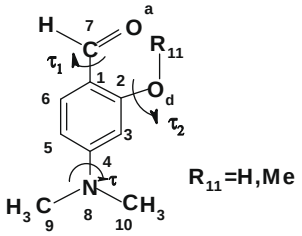

Scheme I. Structure of N,N-dimethylamino orthomethoxy benzaldehyde (PDOHBA, when R_{11} = H) and para-N,N-dimethylamino orthomethoxy benzaldehyde (PDOMBA, when R_{11} = CH_3) with numbering of atoms.

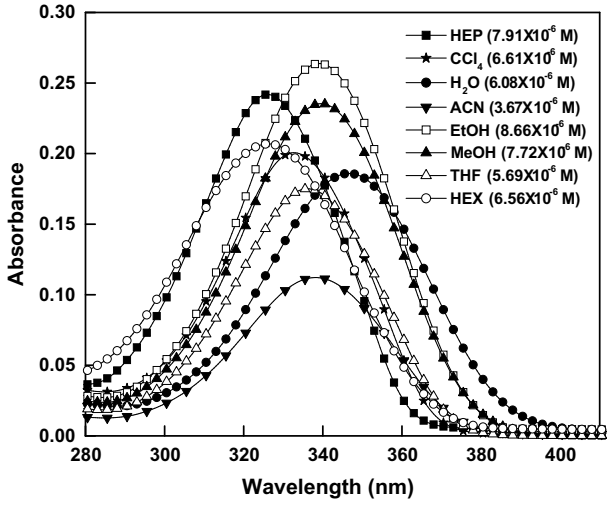

Fig. 1. Absorption spectra of PDOHBA in solvents of varying polarity at room temperature. Concentrations of PDOHBA are given in parentheses.

Table 1
Spectroscopic parameters obtained from absorption and emission measurements of PDOHBA in different solvents at room temperature.

Solvents	Absorption peak (nm)	Emission peak (nm)		Quantum yield (ϕ_K)[a]
		λ_1	λ_2	
MCH	334	–	513	0.55×10^{-2}
CYC	332	–	513	0.49×10^{-2}
HEPT	332	–	512	0.58×10^{-2}
THF	340	400	516	1.00×10^{-2}
CCl_4	338	399	513	0.95×10^{-2}
ACN	341	400	519	0.77×10^{-2}
EtOH	341	403	515	1.26×10^{-2}
MeOH	341	404	515	1.33×10^{-2}
MeOH + acid	341	404	510	–
MeOH + base	352	–	488	–
H_2O	348	404	518	0.60×10^{-2}

[a] Quantum yield for the most red sided band (~515 nm).

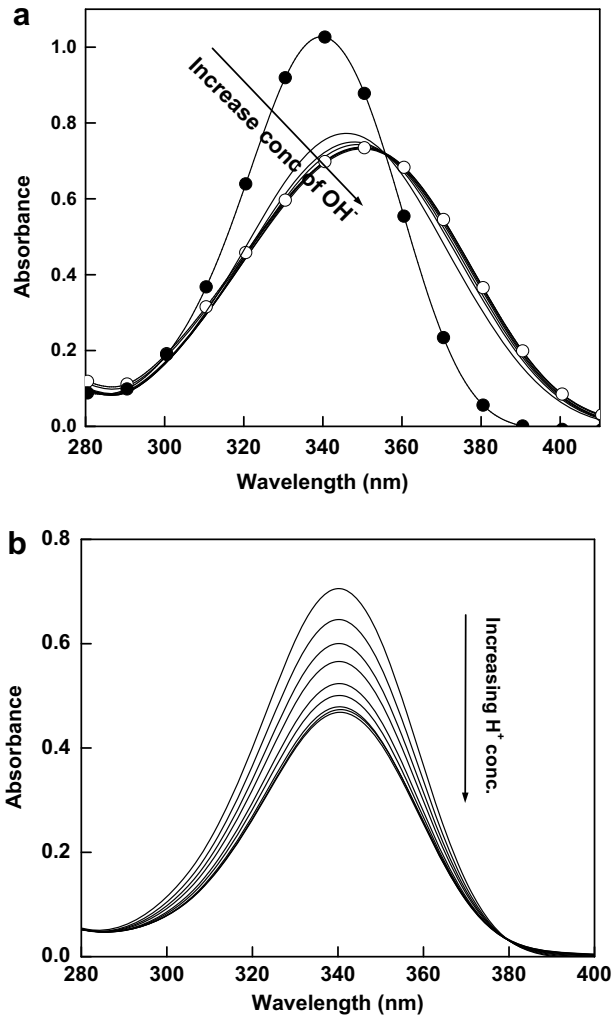

Fig. 2. Variation of the absorption spectra on addition of (a) base (NaOH) and (b) acid in the methanolic solution of PDOHBA at room temperature. Arrow indicates increase of base or acid concentration.

main interest is to study the possible excited state CT and PT reaction for this molecule. The photophysical properties of the molecule have been investigated using steady state absorption and emission spectroscopy and time resolved emission spectroscopy. Side by side quantum chemical calculations at Hartree Fock (HF) [59] and Density Functional Theory (DFT) [60,61] levels have been performed to study the ground and excited state properties of the molecule. Potential energy surfaces (PESs) along the proton transfer and charge transfer coordinates have been evaluated for both the ground and excited states and the theoretical spectral findings have been correlated with experimental absorption and emission spectra.

2. Experimental

2.1. Materials

The molecule PDOHBA was synthesized with simple literature procedure. The molecule $POCl_3$ (1.5 eqv.) was added slowly in dry DMF at 0 °C and stirred for another 30 min. Then m-dimethylaminophenol in dry DMF was added to the reaction mixture at 0 °C and then slowly warmed to room temperature and stirred for another 2 h. Then the reaction mixture was poured into ice cold water and extracted with dichloromethane. The organic layer was washed with water and brine and dried over anhydrous sodium sulphate. The solvent was removed under vacuum to get PDOHBA. ^{1}HNMR (300 MHz, $CDCl_3$): δ 3.05 (s, 6H, NMe_2), 6.06 (d, 1H, J = 2.1 Hz), 6.27 (dd, J = 2.2 Hz, 8.85 Hz, 1H), 7.28 (d, J = 8.8 Hz, 1H), 9.50 (s, 1H), 11.59 (brd. 1H).

2.2. Absorption and emission measurement

The absorption and emission spectra were taken by Hitachi UV–vis (U-3501) spectrophotometer and Perkin Elmer (LS-50B) fluorimeter, respectively. In all measurements, the sample concentration was maintained within the range 10^{-4}–10^{-6} mole/dm^3 in order to avoid aggregation and re-absorption effects. In all cases solvent correction has been done for the measurement of excitation and emission spectra. Fluorescence life time measurements have been done by usual time correlated single photon counting technique (TCSPC). The TCSPC setup was from Edinburgh instruments, UK. An excitation laser source of wavelength 375 nm (instrument response function = 73 ps) was used to excite PDOHBA [62].

2.3. Theoretical calculations

For the ground state, all possible low energy structural isomers of PDOHBA were computed using Hartee Fock (HF) and density functional theory (DFT) methods using GUASSIAN 03 software [63]. All structural parameters for the ground state lowest energy conformer have been calculated at the same level. Potential energy curves (PECs) have been constructed along the proton transfer coordinate from proton donor (hydroxyl group) to the acceptor (aldehyde group) site [18–20]. The ground state (S_0) intramolecular proton transfer (GSIPT) curves were computed using the energies of the B3LYP/6-31++G** fully optimized geometry at fixed O_d–H_{11} distances over the range of 0.90 Å–1.8 Å (Scheme I). The singlet excited states (i.e., S_1 and S_2) potential energy curves along the proton transfer coordinates were obtained by calculating the Franck–Condon transition energies for each of the B3LYP/6-31++G** ground state structures at the Time Dependent Density Functional Theory (TDDFT) level [64]. The Franck–Condon curves for the proton transfer process are obtained by adding the TDDFT/6-31++G** excitation energies to the corresponding ground state energy obtained from the GSIPT curves. Although optimization of the excited state geometry at each O_d–H_{11} distance may provide better insight of excited state surface, but the present approach has been successfully used to evaluate the excited state surfaces for proton transfer reaction in several recently studied systems [18–20,65]. For the three dimensional plot, we have used the same procedure for all the states except we have varied O_d–O_a bond distance in addition to O_d–H_{11} distance. For the charge transfer process, the theoretical PECs for the ground and first ex-

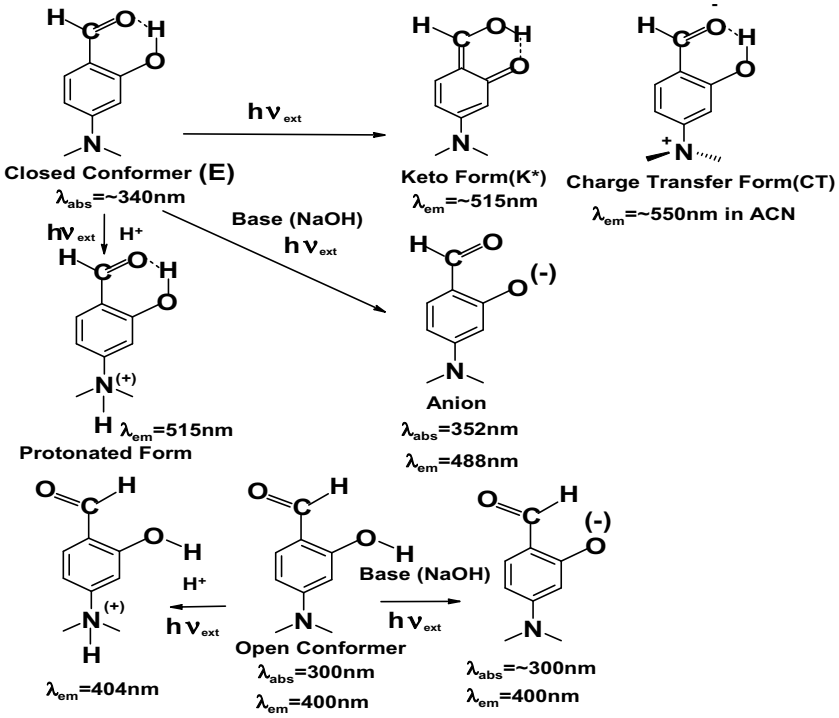

Scheme II. Different species of PDOHBA present in the ground and excited states.

cited singlet states have been explored following the twisted intramolecular charge transfer model as proposed by Grabowski et al. [22,23]. So far there are different ways of calculating the ground and excited state surfaces for the donor–acceptor CT systems [66,67]. During the evaluation of the ground state potential energy surface full geometry optimization is performed at different τ (Scheme I) values ranging from $-10°$ to $130°$. For the construction of excited state curves for both the processes, the vertical excitation energies calculated by TDDFT/6-31++G** method is added to the ground state energy. The TDDFT method of calculation using GAUSSIAN 03 does not implement analytical gradients within TDDFT and hence it fails to optimize the geometries for the excited states [63]. However, the results obtained using this method correlates well with the experimental data [65].

3. Results and discussions

3.1. Absorption spectra

The absorption spectra of PDOHBA measured in different organic solvents such as non-polar, polar aprotic and polar protic solvents at room temperature are shown in Fig. 1 and the position of the spectral band maxima are presented in Table 1. As seen from Fig. 1, the single broad absorption maxima exhibited by PDOHBA shifts slightly to the red side with increasing solvent polarity and hydrogen bonding ability. For non-polar solvents the absorption maxima is at ~332 nm and it shifts to ~348 nm in polar solvents such as water (Table 1). Out of two basic subunits in PDOHBA, it is reported that the CT unit containing DMABA molecule shows its absorption peak at ~337 nm for its π–π^* transition [57]. On the other hand, the PT unit OHBA shows its absorption band at 350 nm (strong) and 330 nm (weak) for π–π^* transition of the closed and solvated open form, respectively [50,51]. The absorption band for the π–π^* transition of PDOHBA is red shifted due to more resonance stabilization compared to that of the pure benzene chromophore. The strong absorption band indicates the existence of conformer with high abundance in the ground state. That species may be the lowest energy intramolecularly hydrogen bonded closed conformer as seen in Scheme I. As was seen in case of OHBA molecule, the closed conformer of PDOHBA is stabilized in the ground state by strong intramolecular hydrogen bond between the hydrogen of hydroxyl (–OH) group and oxygen of aldehyde (–CHO) group. Apparently, the strong π–π^* transition of PDOHBA correlates well with the absorption peaks of two subunits. However, OHBA molecule shows a weak shoulder band at ~330 nm towards the blue side of the strong band for its solvated open form

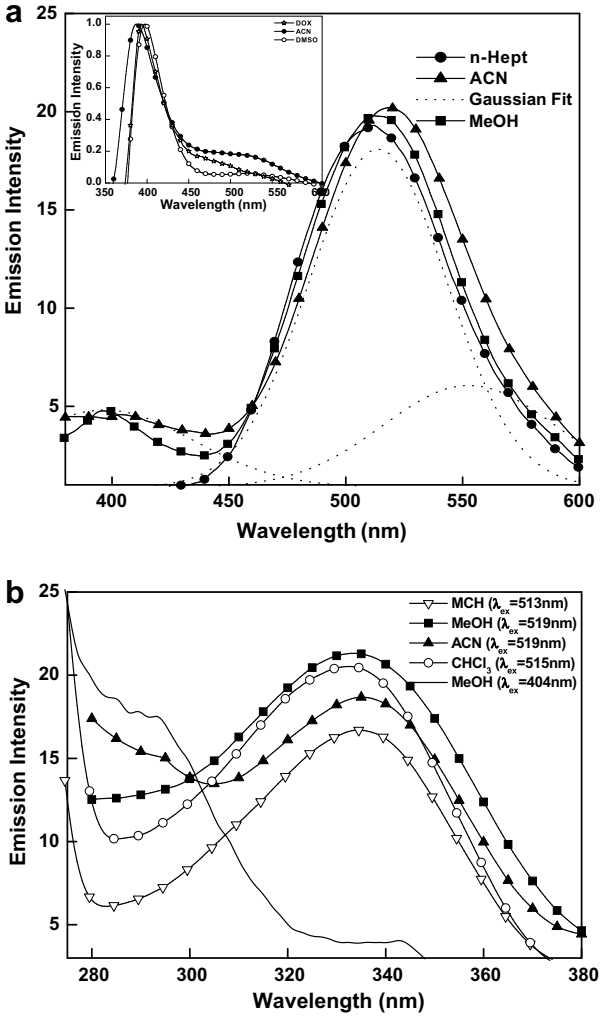

Fig. 3. (a) Emission spectra of PDOHBA in solvents of varying polarity at room temperature (λ_{ext} = ~335 nm). Dotted lines are the deconvolution of emission curve obtained in ACN solvent. Inset: emission spectrum of PDOMBA in different polar-aprotic solvents (λ_{ext} = ~335 nm). (b) Excitation spectra of PDOHBA in different solvents monitored at lower and higher wavelength emission band.

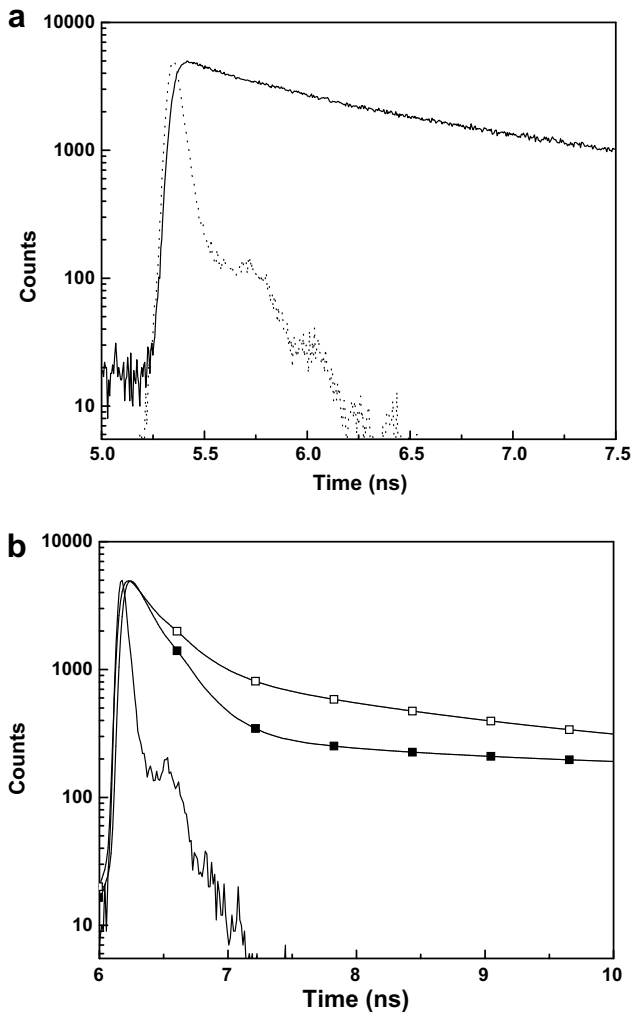

Fig. 4. Fluorescence decay curve of PDOHBA in (a) non-polar and (b) in ACN (-□-) and methanol (-■-) solvent (λ_{emi} = 521 nm, λ_{ext} = 375 nm).

[50,52–54]. Although the absorbance value is high at 330 nm, but a distinct peak is not observed for PDOHBA molecule. At this stage, therefore, it is difficult to predict about the presence of the less abundant solvated open form of PDOHBA molecule as was seen in case of OHBA. The absorption maxima is slightly red shifted with the solvent polarity and hydrogen bonding ability because there may be a little charge separation between the donor ($-NMe_2$) and the acceptor (–CHO) groups of PDOHBA in the excited state.

3.2. Effect of acid and base on absorption spectra

The absorption spectra of PDOHBA in methanol do not change in presence of electron donor weak base triethylamine (TEA). On the other hand, when we add strong base such as NaOH in the methanolic solution of PDOHBA the absorption maxima is red shifted to ~352 nm with concomitant decrease in absorbance value (Fig. 2a). The position of absorption maxima of OHBA in EtOH solvent is shifted on addition of base and the new red-shifted band was assigned to the anion of OHBA in the ground state. Thus, the new band at ~352 nm in the absorption spectra is undoubtedly assigned to the anion of the closed conformer of PDOHBA (Scheme II). In the ground state, the strongly hydrogen bonded closed conformer does not allow weak base TEA to form anion. However, strong base NaOH can easily break the intramolecular hydrogen bond and forms anion in polar solvents but fails to form the anion in non-polar media, probably due to the presence of strong intra-

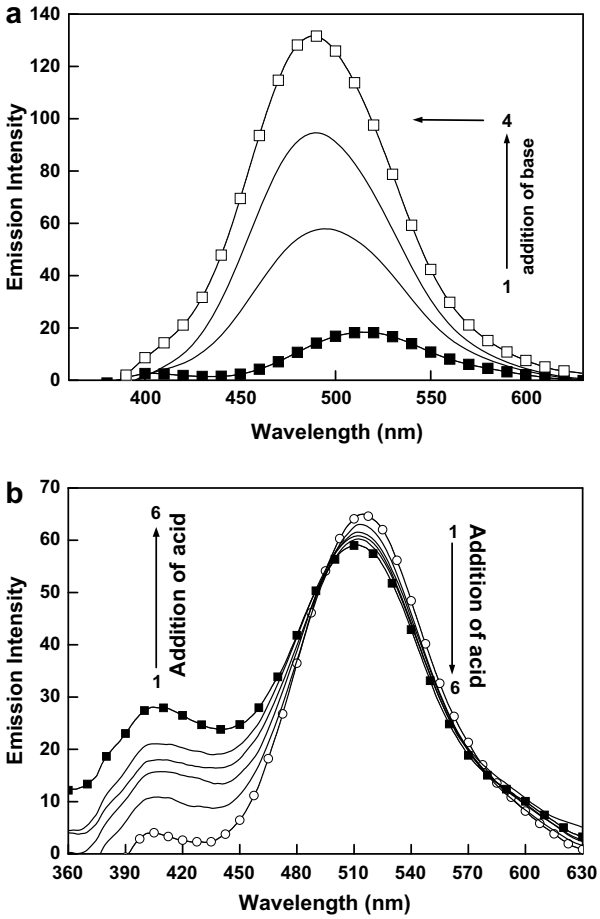

Fig. 5. Emission spectra on addition of (a) base (NaOH) (λ_{ext} = 352 nm): (1) without base and (2–4) with increasing base concentration and (b) acid (λ_{ext} = 341 nm) in the methanolic solution of PDOHBA at room temperature: (1) without acid (2–6) with increase acid concentration.

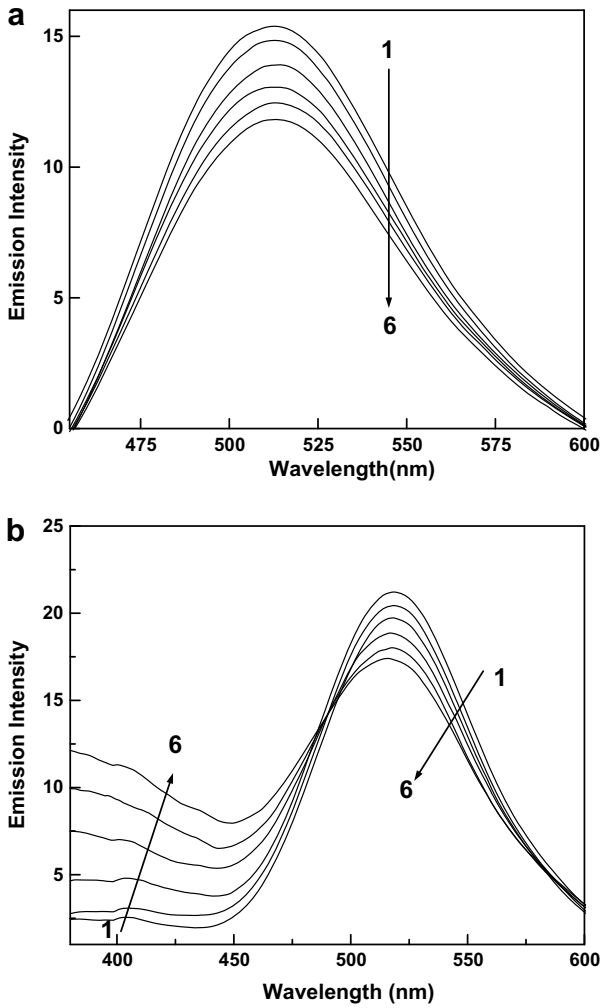

Fig. 6. Effect of temperature on the emission spectra of PDOHBA in (a) methyl cyclohexane and (b) methanol above room temperature. (1) 298, (2) 303 (3) 308, (4) 313, (5) 318, and (6) 323 K.

Table 2
The calculated ground and excited state optimized parameters of PDOHBA for the E- and K-form ($R_{O_d}-H_{11}$ = 1.600 Å) at HF/6-31++G** and DFT (B3LYP/6-31++G**) levels in the gaseous phase. Bond distances and bond angles are given in Å and degree, respectively.

Parameters	*E*	*E*[a]	*K*	*K*[a]
O_d-H_{11}	0.953 (0.992)	0.962	1.600 (1.600)	1.600
O_a-H_{11}	1.881 (1.729)	1.774	0.986 (1.025)	0.981
C_1-C_2	1.408 (1.426)	1.478	1.465 (1.473)	1.478
C_2-C_3	1.384 (1.393)	1.362	1.426 (1.423)	1.424
C_6-C_1	1.411 (1.406)	1.406	1.436 (1.432)	1.423
O_d-O_a	2.697 (2.623)	2.626	2.482 (2.531)	2.492
N_8-C_4	1.362 (1.373)	1.365	1.359 (1.372)	1.397
C_9-N_8	1.449 (1.457)	1.449	1.453 (1.459)	1.446
$C_{10}-N_8$	1.449 (1.457)	1.453	1.451 (1.458)	1.456
C_1-C_7	1.450 (1.440)	1.440	1.361 (1.381)	1.383
$\angle O_d-H_{11}-O_a$	141.99 (147.90)	145.77	147.72 (149.80)	148.89
$\angle C_2-O_d-H_{11}$	110.34 (107.24)	110.07	103.14 (101.99)	103.69
$\angle C_9-N_8-C_4$	120.55 (120.57)	120.47	121.78 (121.48)	117.44
$\angle C_{10}-N_8-C_4$	120.23 (120.13)	110.07	119.44 (119.54)	116.61
$\angle C_1-C_7-O_a$	124.46 (124.46)	123.63	124.05 (123.89)	123.07
$\angle C_9-N_8-C_4-C_5$	−0.08 (−0.06)	−4.83	0.68 (0.71)	−10.72
$\angle C_{10}-N_8-C_4-C_3$	0.07 (0.12)	20.93	−0.11 (0.70)	−56.82
Dipole moment	5.931D (6.441D)	6.172D	6.212D (6.214D)	5.470D

[a] Values in the parenthesis obtained at DFT/B3LYP/6-31++G** level.

molecular hydrogen bonding in these non-interfering solvents. As was observed in case of OHBA, if the less abundant open solvated form of PDOHBA is present in the system it can also form its anion upon addition of strong base. But the strong absorption peak for the anion of the closed conformer may mask the weak anion band of the open solvated from.

At room temperature, gradual addition of dilute H_2SO_4 to the methanolic solution of PDOHBA does not shift the absorption maxima but shows a decrease of the absorbance (Fig. 2b). Strong acid can rupture IMHB and the H^+ ion of acid can bind to the lone pair of nitrogen. As the absorption spectral position is not changed, we could say that the protonated species of both the conformers absorbed at the same position of the neutral species. It is to point out here that protonation at the nitrogen centre for donor–acceptor CT systems usually shifts the absorption maxima to the blue due to less resonance stabilization of the protonated species than their neutral counterpart [26–29].

3.3. Fluorescence emission and excitation spectra

Emission and excitation spectra of PDOHBA have been taken in different solvents at room temperature and are shown in Fig. 3a and 3b, respectively. All the spectral data are presented in Table 1, and the spectral observations are summed up below. It is seen that PDOHBA exhibits a large Stokes shifted fluorescence in all non-polar hydrocarbon solvents and dual fluorescence bands in polar solvents. In non-polar hydrocarbon solvents, for example in cyclohexane, PDOHBA exhibits a broad structureless emission band at ~513 nm upon excitation at ~334 nm. Two emission bands of PDOHBA are observed at ~515–518 nm range (broad) and at around 402 nm in polar solvents. Like the absorption spectra, the low energy (~515–518 nm) emission band of PDOHBA apparently undergoes a slight bathochromic shift with increasing solvent polarity at room temperature (Fig. 3a). Interestingly in non-polar solvents the broad emission band at ~513 nm is quite similar to that observed for OHBA in non-polar media. Nagaoka et al. [52] observed a single emission band of OHBA at ~510 nm in non-polar solvents at room temperature. It is reported that OHBA shows dual emission band due to emission from LE state of open solvated form (~420 nm) and PT form of the closed form (~520 nm) in EtOH solvent [50]. Unlike OHBA, methyl salicylate (MS) exhibits dual emission in non-polar solvents. This was interpreted by considering higher energy barrier for the keto–enol tautomerism in MS compared to that of OHBA. Experimentally, it is found that in case of MS the energy barrier for this keto–enol tautomerism in the excited state lies in the range of ~3.7–4.7 kcal/mole in methylcyclohexane solvent whereas that obtained for OHBA is ~1.7 kcal/mole and hence OHBA shows only PT emission. It is reported that the donor–acceptor CT molecule DMABA shows only local emission (~400 nm) in non-polar solvents and dual fluorescence in medium to highly polar solvents for the LE (~400 nm) and CT (~537 nm) emissions [57]. The CT emission in DMABA is found to be dependent of solvent polarity. Therefore, the red shifted less polarity sensitive band insists us to assign it as only proton transfer emission band. However, it is important to note that emission spectrum of PDOHBA in ACN solvent is found to be composed of three bands (Fig. 3a). These three bands are at ~400, ~513 and ~550 nm. The most red-shifted emission band at ~550 nm is more or less similar to the emission spectra of DMABA [57]. To confirm this assignment with an additional support we have intentionally synthesized para-N,N-dimethylamino ortho methoxy benzaldehyde (PDOMBA) and studied its absorption and emission spectra. As the hydroxyl hydrogen of PDOHBA is replaced by methyl group to form PDOMBA (Scheme I) there is no question of PT process, and only CT process is expected in the excited state. Interestingly, PDOMBA shows solvent polarity dependent CT emission (λ_{em} = ~550 nm in ACN solvent) (Fig. 3a inset). Therefore

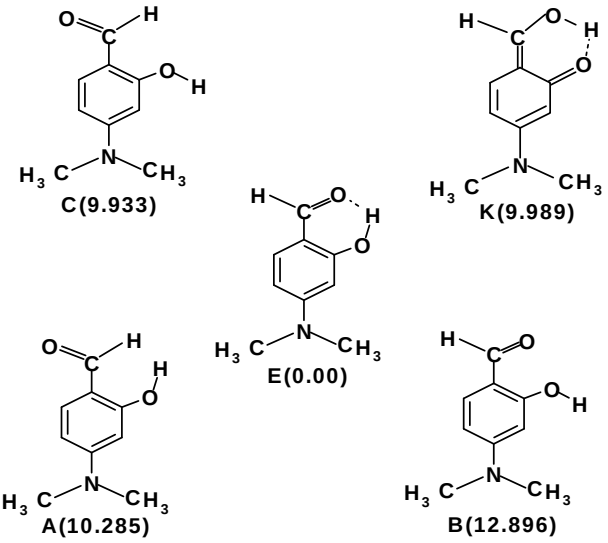

Chart I. Different ground state conformers of PDOHBA obtained at DFT level. Energies (kcal/mole) are given with respect to the lowest energy E form.

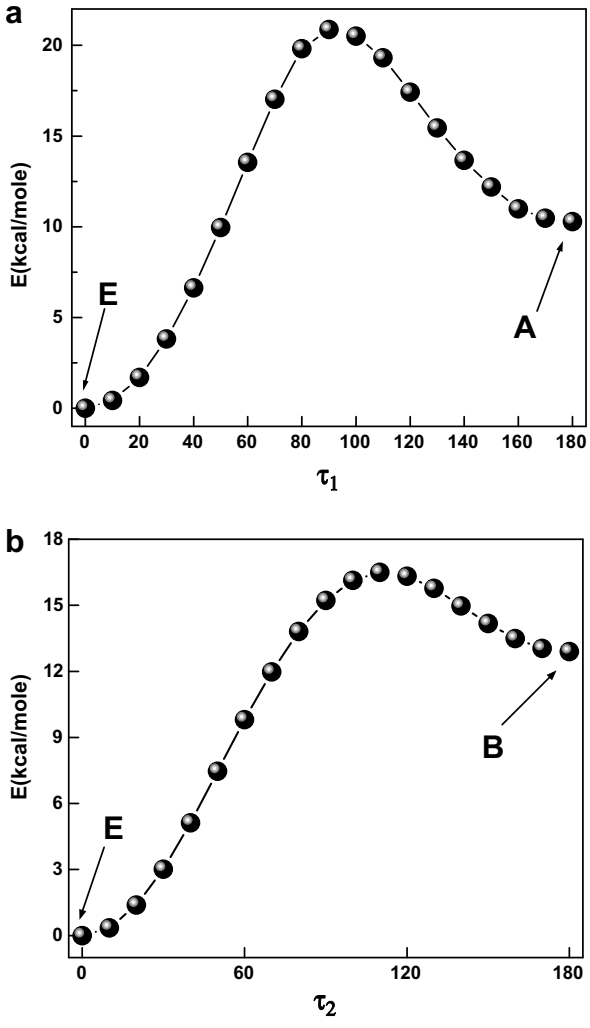

Fig. 7. Variation of energy during the transformation from (a) E to A form and (b) from E to B form of PDOHBA by twisting of angle τ_1 and τ_2, respectively, at DFT level using 6-31++G** basis set and B3LYP functional.

the red-shifted emission band at ~518 nm of PDOHBA is assigned to PT emission and is similar to PT emission of OHBA. And the most red sided emission band at ~550 nm of PDOHBA is the CT emission and is similar to that of DMABA. Overall the assignment of PT and CT emission bands is correct and meaningful and is further confirmed from lifetime measurements. As shown in Fig. 3b, the excitation spectra monitored at the lower energy band bears resemblance to the absorption spectra in all non-polar, polar protic and aprotic solvents. But the excitation spectra monitored at the higher energy emission band (402 nm) is slightly blue shifted and this corresponds to solvated open form. So this higher energy band probably arises from the conformer of PDOHBA which may have minor existence in the ground state. The emission from the open solvated form is low due to little existence in the ground state as it is higher in energy compared to the hydrogen bonded stabilized closed conformer of PDOHBA. Very similar observation was found by Nagaoka et al. for OHBA molecule in polar protic solvents.

The fluorescence quantum yields (Table 1) of the Stokes shifted emission band of PDOHBA in different solvents were measured by secondary standard method using β-naphthol in methylcyclohexane ($\phi_f = 0.23$) [20]. It is found that the relative quantum yields for the red-shifted band is quite high compared to that of the normal emission. In case of non-polar solvents, only K^*-form exists and its quantum yield is low (0.005) compared to that of polar solvents. This may be due to the absence of minima for the K-form in the ground state (see theoretical results).

3.4. Fluorescence lifetime measurement

Fluorescence lifetime measurements can provide useful information about the excited state of a molecule. The fluorescence lifetime of the low energy emission band (515 nm) of PDOHBA is found to be single exponential in case of non-polar solvent (heptane) and its lifetime value is 0.27 ns and the corresponding χ^2 value is 1.05 (Fig. 4). But in case of polar solvents like ACN and MeOH, the fluorescence decay curve are, however, biexponential in the wavelength region of ~521 nm. A decay time of 0.22 ns (80%) and ~3.62 ns (20%) are obtained in ACN solution at room temperature. In methanol solvent, the fluorescence decay of same band is found to be ~0.19 and 1.4 ns. It is reported that the fluorescence lifetime for the PT band of OHBA is ~44 ps in non-polar solvents [50] and that of the CT band of DMASAME is 7.2–12.6 ns in ACN medium [52]. Comparing the fluorescence decay of PDOHBA with OHBA and DMASAME we can assign the faster decay component to PT emission and slower decay component to CT emission. We can also say that in non-polar solvents the single emitting species is the PT form of PDOHBA. In case of polar solvents there are two emitting species; PT contribution is more than the CT emitting species at ~521 nm. Overall we can say that the molecule PDOHBA exhibits proton transfer in non-polar solvents and both proton transfer as well as charge transfer in polar solvents. This is well supported by theoretical calculation.

3.5. Effect of acid and base on emission spectra

Both the increase and decrease of pH has remarkable effect on the spectral properties of PDOHBA. Gradual addition of aqueous solution of NaOH to methanolic solution of PDOHBA results in a blue shift of the emission maxima of the lower energy band to ~488 from 515 nm (Fig. 5a). In methanol solvent, the excitation spectrum for ~488 nm emission band in basic medium correlates

Table 3
IR data and experimental intramolecular hydrogen bond strength in the ground state of PDOHBA and OHBA Theoretical ((DFT/B3LYP/6-31++G**) stretching frequency of O–H and C=O modes are in parenthesis.

Compound	ν_{O-H} (cm^{-1})	$\Delta\nu_{O-H}$ (cm^{-1})	$\nu_{C=O}$ (cm^{-1})	$\Delta\nu_{C=O}$ (cm^{-1})	K_{IMHB} (kcal/mole)
PDOHBA	3439(3316)	179[a]	1644(1698)	65[b]	9.84
OHBA	3160	451[a]	1668	41[b]	6.12

[a] The displacement of the OH frequency from the position (3611 cm^{-1}) in phenol [69].
[b] The displacement of C=O frequency from the position (1709 cm^{-1}) in benzaldehyde [70].

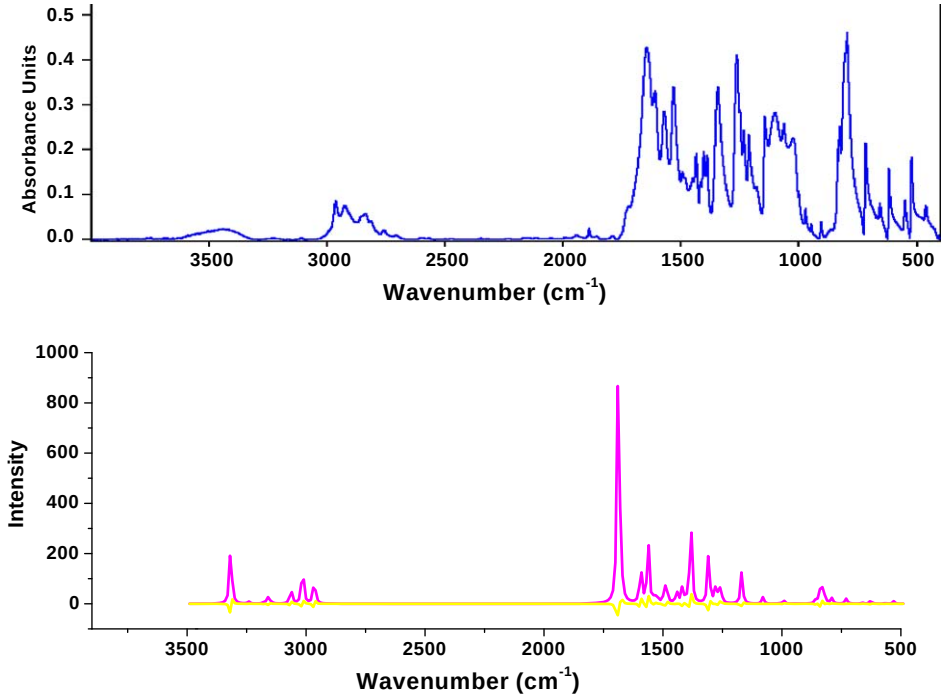

Fig. 8. Experimental (upper) and calculated (B3LYP/6-31++G**) IR spectra (lower) for the lowest energy conformer of PDOHBA.

well with the absorption spectrum of PDOHBA in basic medium with band at ~352 nm. Thus the emission band at ~488 nm is assigned to the anion of the closed conformer (Scheme II), which is formed due to abstraction of proton by the addition of base. Similar effect is observed in all polar protic solvents. The large Stokes shifted fluorescence of the anion is attributed to its capability of resonance stabilization by extensive delocalization of the negative charge over the benzene π-electrons. Base has no effect on the emission spectra of PDOHBA in non-polar solvents. This is probably due to the presence of strong intramolecular H-bonding in PDOHBA in non-polar solvents, which cannot be ruptured even by strong base. It is to point out that OHBA molecule shows a strong (490 nm) emission peak for the anion of the closed conformer. As seen in Fig. 5a, a weak blue sided emission band is observed and is assigned to the anion of the open form.

Addition of dilute H_2SO_4 in MeOH solution of PDOHBA results in increase in intensity of the higher energy band (~404 nm) with a concomitant decrease in the intensity of the lower energy band (~515 nm). The lower energy band shifts to blue from 515 to 510 nm showing a clear isoemissive point at ~495 nm (Fig. 5b). This indicates the presence of equilibrium between the two species. Thus, the emission band at 515 nm corresponds to the protonated species of the closed form and the band at 404 nm corresponds to the protonated species of the open form. Very similar observation was found in case of OHBA molecule. Although the weak absorption and emission band for the less abundant solvated open form is not distinguishable from the strong band of the highly abundant closed conformer, but the emission from the protonated open form is clearly distinguishable. The kinetic scheme is shown in Scheme II.

3.6. Effect of temperature on emission spectra

The variation of temperature has pronounced effect on the emission spectra of PDOHBA in both polar and non-polar solvents. The effect of temperature further reinforced our assignment of different emitting species.

In case of non-polar solvents such as cyclohexane, the lower energy emission band at ~513 nm shows a decrease in intensity with increasing temperature and may be due to the increase of non-radiative deactivation channels. However, the position of the emission maxima remains unchanged throughout (Fig. 6a). As seen in Fig. 6b, in case of polar protic solvents, with increase of temperature, the lower energy emission band at ~515 nm shows a decrease in intensity and a concomitant increase in intensity of the higher energy band at ~404 nm of PDOHBA. It is interesting that the enhancement of the emission intensity of higher energy band is only observed above room temperature. Similar observation was found in polar aprotic solvents too. This could be due to greater population of higher energy species (open form) at high temperature which emits at higher energy side. Very similar observation was reported in case of OHBA [43].

3.7. Quantum chemical calculations

3.7.1. Structural calculations and intramolecular hydrogen bond in the ground state

The structural calculations have been performed by DFT and HF levels using GAUSSIAN 03 software [63]. The structural parameters of the two low energy conformers of PDOHBA molecule are explored in the electronic ground state by HF method using 6-

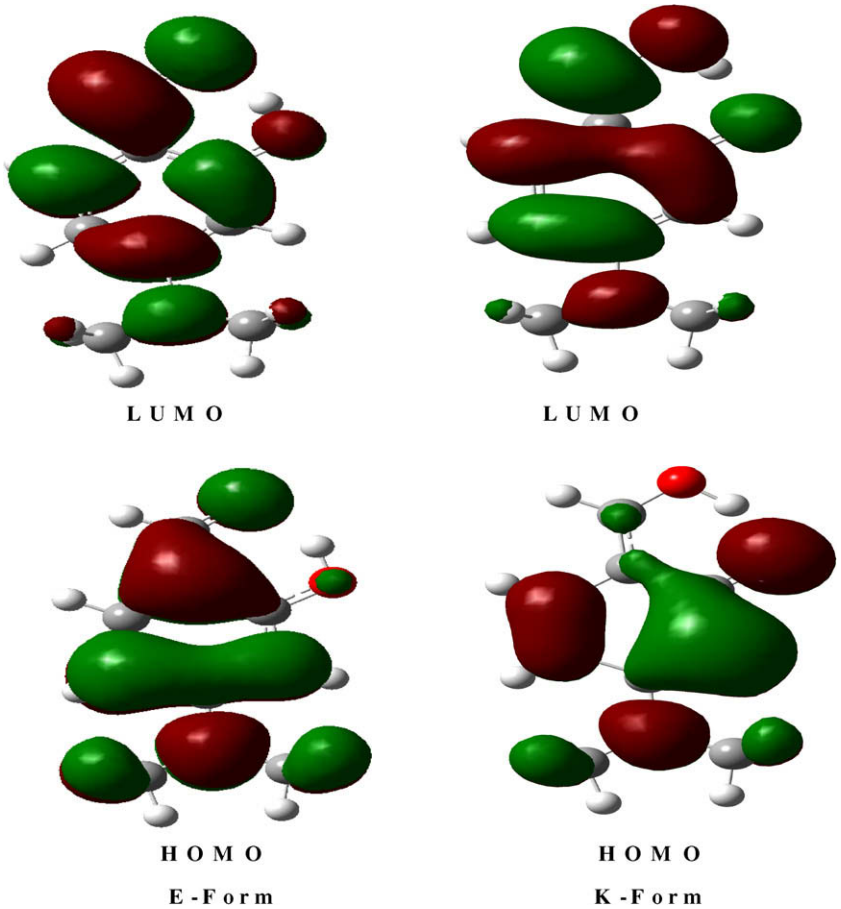

Fig. 9. The HOMO and LUMO orbitals which are involved in the electronic transition from S_0 to S_1 of E-tautomer and K-tautomer ($R_{O_4-H_{11}} = 1.6$ Å).

31++G** basis set and DFT method using B3LYP functional and 6-31++G** basis set and the structural parameters for the enol (E) and keto (K) forms are presented in Table 2. Different low energy computed structures with respect to the position of hydroxy and aldehyde group for the ground state is shown in Chart I. Out of all the possible structures it is seen that the intramolecularly hydrogen bonded closed form (E-form) is more stable than any other forms of PDOHBA molecule. Intramolecular hydrogen bonding also stabilizes the K-form compared to any of the open conformers except conformer C (Chart I).

As seen in Fig. 7, the DFT level of calculations yield energies (E in kcal/mole) for different electronic states with the variation of torsional angle (τ) at the hydroxyl and aldehyde sites separately. The strength of IMHB (E_{IMHB}) for the A form has been determined to be 10.29 kcal/mole by rotating the aldehyde (–CHO) group out of the H-bonded configuration and computing the energy difference between closed (E-form) and open form (A-form) (Fig. 7a). Similar calculation has been carried out by rotating the phenolic OH group out of the H-bonded configuration and the strength of IMHB (E_{IMHB}) for E-form is determined to be 12.90 kcal/mole (Fig. 7b).

In order to evaluate the intramolecular hydrogen bond strength (E_{IMHB}) the IR spectra of PDOHBA has been recorded and is shown in Fig. 8. Table 3 shows the characteristic IR frequencies (ν_{O-H} and $\nu_{C=O}$ stretching) of PDOHBA and OHBA. Theoretical IR spectra (Fig. 8) has been calculated at B3LYP/6-31++G** level for the lowest energy intramolecular hydrogen bonded closed conformer of the molecule. It is well known that IMHB formation gives rise to a red shift of the ν_{O-H} frequency compared to a typical free OH stretching frequency. It is found that for molecules PDOHBA and OHBA, the O–H stretching frequency (ν_{OH}) appears at remarkably lower frequency compared with those of phenol and the C=O stretching frequency ($\nu_{C=O}$) decreases significantly relative to that of benzaldehyde [68]. According to Zadorozhnyi and Ishchenko method the hydrogen bond energy (E_{IMHB}) can be evaluated from the following relation [69,70]:

$$\frac{\Delta\nu_{C=O}}{\nu_{C=O}} = -K_{C=O}E_{IMHB}, \quad (1)$$

where $\Delta\nu_{C=O}$ and $K_{C=O}$ are the magnitude of the spectral shift of C=O stretching mode and proportionality coefficient reported to be 9.6×10^{-4} mole/kJ [70]. From the above relation, the calculated E_{IMHB} of PDOHBA and OHBA are 9.84 and 6.12 kcal/mole, respectively (Table 3), indicating stronger hydrogen bond in PDOHBA than OHBA. Therefore, the calculated E_{IMHB} of PDOHBA from IR data is found to be comparable with the values obtained by DFT level calculations. High electron donating ability of $-NMe_2$ group is responsible for such effect in PDOHBA.

3.7.2. Proton transfer and charge transfer processes and PESs

The optimized parameters for the ground and the excited state geometry using 6-31++G** basis set at the Hartee Fock (HF) and CIS levels respectively, are shown in Table 2. It is seen from the calculated data that the O_d–H_{11} bond length increases from 0.953 to 0.962 Å from ground state (GS) to the excited state (ES). Similarly, the $O_d \ldots H_{11} \ldots O_a$ bond angle increases from 141.99° to 145.77° and $O_d \ldots O_a$ bond distance decreases from 2.697 Å to 2.626 Å from ground to the excited state. Interestingly, the $O_d \ldots H_{11} \ldots O_a$ bond angle (147.72°) and $O_d \ldots O_a$ bond distance (2.482 Å) for the K-form is closer to the corresponding excited state parameters of the E*-form. Therefore, this structural change of bond length and bond angle in going from ground to the excited state indicates possible proton transfer in the excited state to generate the K-form having geometrical parameters at the cyclic intramolecular hydrogen bonding site similar to that of E*-form. It is pertinent to point out here that structurally, the nitrogen centre is twisted at the excited state compared to that of the planar structure in the ground state. Such pre-twisted geometry usually favours ICT process as per TICT model [23]. Examination of the computed negative charge distribution from Mulliken Scheme at HF/6-31++G** level shows an increase of negative charge distribution on O-atom of C=O group from ground to the excited state (−0.579 in GS to −0.594 in ES). Simultaneously negative charge distribution decreases on O-atom of –OH group (−0.621 in GS to −0.602 in ES). This also supports the possibility of proton translocation from –OH group to –CHO group of PDOHBA on excitation. It is probable that on excitation PDOHBA attains a delocalized excited state, which then relaxes to the proton transferred configuration with the transfer of proton from –OH group to –CHO group. The change in dipole moment from ground to the excited state for both the E- and K-form is not significant (Table 2). Therefore, theoretically it can be said that the solvent dependency of the red-shifted emission band should be very less. In fact, experimentally it is found that the position of red-shifted emission band is practically insensitive to solvent polarity (Table 1).

The HOMO and LUMO orbital for the E- and K- forms are shown in Fig. 9. For both the E- and K- ($R_{O_d-H_{11}}$ = 1.6Å) forms, the HOMO and LUMO are of π and π^* character, respectively. The HOMO of

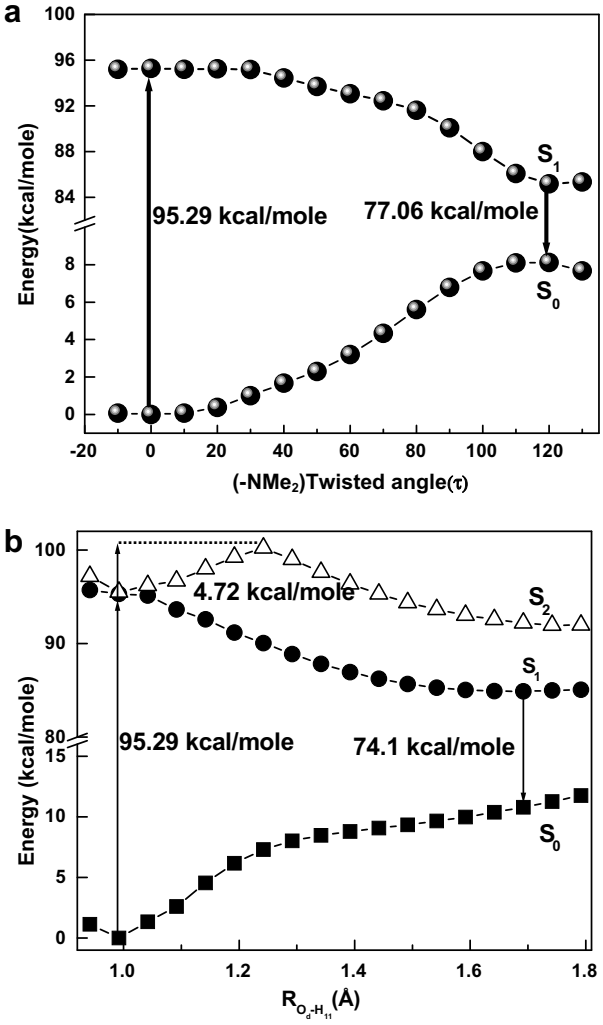

Fig. 10. (a) Potential energy curves for ground and first excited singlet state of PDOHBA with varying of donor ($-NMe_2$) twist angle (τ) in vacuo (Scheme I) calculated at DFT and TDDFT (B3LYP/6-31++G**) level, respectively. (b) Energy variation along the $R_{O_d}-H_{11}$ bond from enol to keto tautomer of PDOHBA for the ground (S_0) and two excited states (S_1 and S_2) calculated at DFT and TDDFT (B3LYP/6-31++G**) level, respectively.

E-form shows antibonding character at C_7–O_d bond region and it has lager electronic projection over O_d atom. There is no electronic projection over the aldehyde group. But in the LUMO of E-form the electronic projection is maximum over O_a of IMHB ring. The HOMO of K-form shows bonding character at C_7–C_9–C_{12} and electronic density projection remains maximum on O_d itself. For the LUMO of K-form the electronic projection increases over O_a compared to LUMO of E-form as well as the HOMO of K-form. Thus, the orbital pictures clearly favour proton transfer in the excited state but not in the ground state.

Fig. 10a represents the variation of potential energy for S_0 and S_1 states along the twisting coordinate (τ; Scheme I). The nature of the plot reflects a barrierless transition from LE to CT form on the S_1 surface in the gaseous phase. For the proton transfer process, we utilized the distinguished coordinate approach with the O_d–H_{11} bond elongation as the primary reaction coordinate for the proton transfer reaction. From Fig. 10b it is seen that the energy of the S_0 state increases with the increase of O_d–H_{11} bond length and there is only single minimum at the enol form in the ground state (S_0). The S_1 state shows an asymmetric double well type potential along the reaction coordinate (O_d–H_{11} bond length), with two minima. In the S_1 state, the K^*-form is more stable than the E^*-form and the proton transfer process is nearly a barrierless process. Experimentally it is seen that in the case of non-polar solvents there is no dual fluorescence, only K^* emission is observed. Therefore, the DFT/TDDFT method is more supportive with the experimental results. The calculated PES for the second excited state (S_2) is an asymmetric double well type. The K^*-form is more stable than the enol form and the enol to keto conversion barrier energy is 4.72 kcal/mole on the S_2 surface. This indicates that proton transfer occurs in the S_1 surface but not of S_0 or S_2 surface.

Investigation of the PEC for the proton transfer reaction needs the specification of a "reaction coordinate" (RC) along which the change of energy will be observed. In our case the RC is the coordinate along which the proton is transferred from O_d to O_a, i.e. the $R_{O_d-H_{11}}$ distance (Chart I). In fact, it has been observed that along with O_d–H_{11} distance the other parameters also undergo a change during the process of proton transfer. As seen in Fig. 11a, it is found that the midway through the proton transfer process, the $O_d \ldots O_a$ distance contracts to a minimum and the angle $O_d \ldots H_{11} \ldots O_a$ increases to a maximum before relaxing to the K-form. A crossover point between E- and K-form is found at around O_d–H_{11} distance of 1.30 Å. All the calculations were done at HF and DFT levels using the 6-31++G** basis set to evaluate S_0 state. In both cases the trend of the plots remains the same. It is interesting to note that the N_8–C_4 bond length decrease with increase OH distance and it shows a minima at O_d–H_{11} distance 1.30 Å (Fig. 11b). Fig. 12 shows the 3D plot for the variation of potential energy with

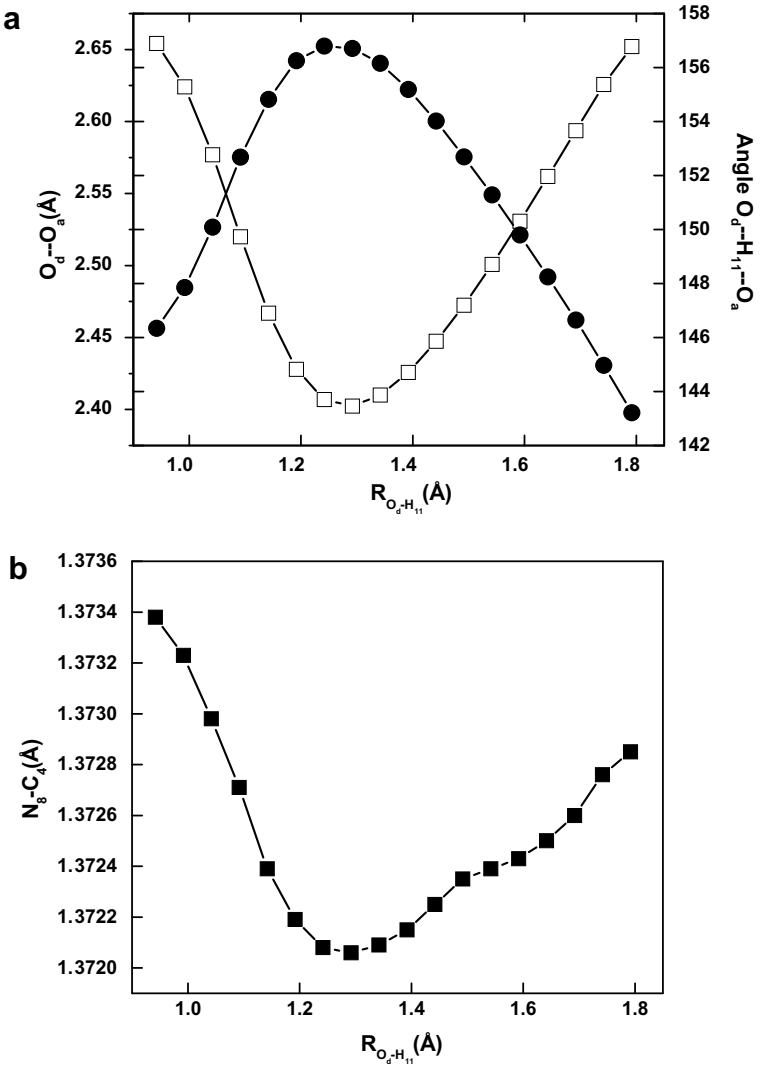

Fig. 11. Variation of (a) $O_d \ldots O_a$ bond distance (-□-) and $O_d \ldots H_{11} \ldots O_a$ bond angle (-●-) with R_{O_d}—H_{11} bond length and (b) N_8-C_4 bond distance at different R_{O_d}—H_{11} bond length at DFT level (B3LYP/6-31++G**).

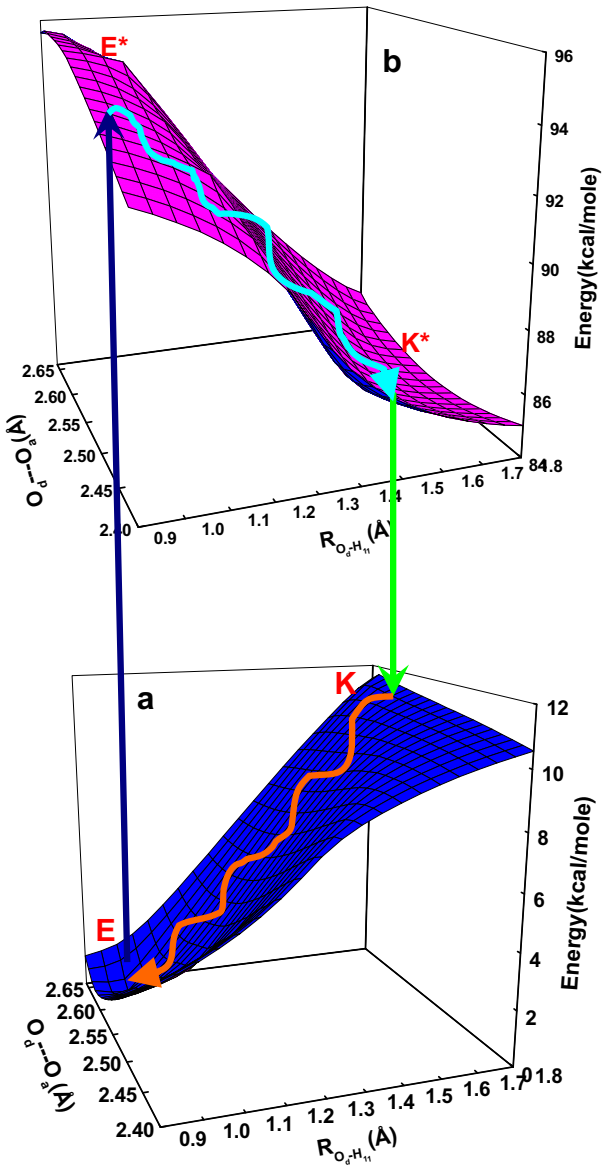

Fig. 12. A 3D plot of variation of energy with respect to change of both $O_d...O_a$ distance and $O_d–H_{11}$ bond length for the (a) ground and (b) excited states at DFT and TDDFT level, respectively.

$O_d–H_{11}$ and $O_d–O_a$ bond lengths for S_0 and S_1 states. As seen in Fig. 12, the transformation from E-form to K-form in the S_0 surface is energetically unfavourable with a single minimum for E-form implying that the E-form is the single existing conformer of PDOHBA in the ground state. On the other hand, on the S_1 surface the transition from E^* to K^*-form is a barrierless process with reversal of stability. In the S_1 state, K^* form is the energetically favourable conformer of PDOHBA unlike the ground state. Very similar results also obtained when 3D plot for the variation of potential energy with $O_d–H_{11}$ bond length and $O_d...H_{11}...O_a$ bond angle for S_0 and S_1 states is performed. Therefore, theoretically the multidimensional plot also supports the feasibility of barrierless excited state proton transfer in PDOHBA and this supports our experimental findings.

4. Conclusion

In this work, we have presented the photophysical properties PDOHBA from spectral measurements and theoretical points of view. The molecule has donor–acceptor charge transfer site resembles to DMABA molecule and proton transfer site resembles to OHBA molecule. Spectral data predict that the molecule shows only excited state proton transfer in non-polar solvents and coupled proton and charge transfer in polar solvents. Hence, the position of the proton transfer emission band is found to be independent of solvent polarity and the Stokes shifted charge transfer emission band shows its dependency on solvent polarity. Fluorescence lifetime measurements also support only excited state proton transfer process in non-polar solvents and combined PT and CT processes in polar solvents. The highly abundant intramolecular hydrogen bonded closed and less abundant open solvated forms generate anion and cation in presence of strong base and acid, respectively, in the ground state. Interestingly, the anion and cation show their independent distinct emission characteristics. The structural aspect of different low energy conformers of the molecule, potential energy surface for proton transfer and charge transfer processes and vibrational modes in PDOHBA have been calculated by using Hartree Fock and Density Functional Theory. The presence of intramolecular hydrogen bond obtained from IR spectrum correlates well with the theoretical IR spectrum. Theoretical potential energy surface support a barrierless proton transfer as well as twisted intramolecular charge transfer reaction in the first excited state of PDOHBA. From experimental and theoretical data it is confirmed that depending upon the nature of solvents, the molecule PDOHBA exhibits only proton transfer or both PT as well as CT reaction in the excited state.

Acknowledgements

NG gratefully acknowledges the financial support received from Department of Science and Technology, India (Project No. SP/S1/PC-1/2003). The authors would like to thank Prof. Tapas Chakraborty and Mr. A. Samanta, IACS, Kolkata for IR measurement The authors are also thankful to Dr. Samir K. Pal and Ajay K. Shaw of S.N. Bose Centre for Basic Science, Kolkata, for allowing them to use fluorescence lifetime measuring instrument. SM and RBS thank CSIR, New Delhi for research fellowship.

References

[1] A.Z. Weller, Electrochem. 56 (1952) 662.
[2] A.I. Sytnik, M. Kasha, Proc. Nat. Acad. Sci. USA 91 (1994) 8627.
[3] S.J. Formosinho, L.G. Arnaut, J. Photochem Photobiol A: Chem. 75 (1993) 21.
[4] A. Douhal, F. Lahmani, A.H. Zewail, Chem. Phys. 207 (1996) 477.
[5] J. Catalan, J.C. Valle, J. Palomar, C. Diaz, J.L.G. Paz, J. Phys. Chem. A 103 (1999) 10921.
[6] S. Lochbrunner, A.J. Wurzer, E. Riedle, J. Chem. Phys. 112 (2000) 10699.
[7] S. Lochbrunner, T. Schultz, M. Schmitt, J.P. Shaffer, M.Z. Zgierski, A. Stolow, J. Chem. Phys. 114 (2001) 2519.
[8] D.G. Ma, F.S. Liang, L.X. Wang, S.T. Lee, L.S. Hung, Chem. Phys. Lett. 358 (2002) 24.
[9] S. Lochbrunner, K. Stock, V. De Waele, E. Riedle, in: A. Douhal, J. Santamaria (Eds.), Femtochemistry, and Femtobiology: Ultrafast Dynamics in Molecular Science, World Scientific, River Edge, NJ, 2002, p. 202.
[10] A.L. Sobolewski, W. Domcke, J. Phys. Chem. A 108 (2004) 10917.
[11] L.M. Tolbert, K.M. Solntsev, Acc. Chem. Res 35 (2002) 19.
[12] P. Leiderman, L. Genosar, D. Huppert, J. Phys. Chem. A 109 (2005) 5965.
[13] S.L. Wang, G.Y. Gao, T.I. Ho, L.Y. Yang, Chem. Phys. Lett 415 (2005) 217.
[14] A.E. Shchavlev, A.N. Pankratov, A.V. Shalabay, J. Phys. Chem. A 109 (2005) 4137.
[15] H. Mishra, S. Maheshwary, H.B. Tripathi, N. Sathyamurty, J. Phys. Chem. A 109 (2005) 2746.
[16] M. Haranczyk, J. Rak, M. Gutowski, D. Radisic, S.T. Stokes Jr., K.H. Bowen, J. Phys. Chem. B 109 (2005) 13383.
[17] A.J.A. Aquino, H. Lischka, C. Hättig, J. Phys. Chem. A 109 (2005) 3201.
[18] S. Mahanta, R.B. Singh, S. Kar, N. Guchhait, Chem. Phys. 324 (2006) 742.
[19] R.B. Singh, S. Mahanta, S. Kar, N. Guchhait, Chem. Phys. 331 (2007) 189.
[20] R.B. Singh, S. Mahanta, S. Kar, N. Guchhait, Chem. Phys. 331 (2007) 373.
[21] E. Lippert, W. Luder, H. Boos, in: A. Mangini (Ed.), Advances in Molecular Spectroscopy, Pergamon Press, Oxford, 1962, p. 443.
[22] Z.R. Grabowski, K. Rotkiewicz, A. Siemiarczuk, D.J. Cowley, W. Baumann, Nouv. J. Chim. 3 (1979) 443.
[23] Z.R. Grabowski, K. Rotkiewicz, W. Rettig, Chem. Rev. 103 (2003) 3899.

[24] N. Mataga, H. Chosrowjan, S. Taniguchi, J. Photochem. Photobiol. C: Photochem. Rev. 6 (2005) 37.
[25] V.A. Galievsky, S.I. Druzhinin, A. Demeter, Y.-B. Jiang, S.A. Kovalenk, L.P. Lustres, K. Venugopal, N.P. Ernsting, N.P. Allonas, M. Noltemeyer, R. Machinek, K.A. Zachariasse, Chem. Phys. Chem. 6 (2005) 2307.
[26] A. Chakraborty, S. Kar, D.N. Nath, N. Guchhait, J. Phys. Chem. A 110 (2006) 12089.
[27] A. Chakraborty, S. Kar, N. Guchhait, J. Photochem. Photobiol. A 181 (2006) 246.
[28] A. Chakraborty, S. Kar, N. Guchhait, Chem. Phys. 320 (2006) 75.
[29] A. Chakraborty, S. Kar, N. Guchhait, Chem. Phys. 324 (2006) 733.
[30] K.A. Zachariasse, T. von der Haar, A. Hebecker, U. Leinhos, W. Kühnle, Pure & Appl. Chem. 65 (1993) 1745.
[31] A.I. Sytnik, J.C. Del Valle, J. Phys. Chem. 99 (1995) 13028.
[32] Y. Kubo, S. Maeda, S. Tokita, M. Kudo, Nature 382 (1996) 522.
[33] L.B. Ferninga (Ed.), Molecule Switches, Wiley-VCH, Weinheim, Germany, 2001.
[34] Memories and Switches. Special issue of Chem. Rev. 100 (2000) 1741.
[35] Ch. Bosshard, K. Sutter, P. Pretre, J. Hulliger, M. Florsheimer, P. Kaatz, P. Gunter, Organic Nonlinear Optical Materials, Adv. Nonlinear Optics, vol. 1, Gordon and Breach, 1995.
[36] J.R. Lakowicz, Principles of Fluorescence Spectroscopy, Second ed., Kluwer Academic, Hongham, 1999.
[37] B. Kippelen, H.S. Lackritz, R.O. Claus, Organic Nonlinear Optical Material and Devices, P. A. Materials Research Society, 1999.
[38] F.-Y. Wu, Z.-J. Ji, Y.-M. Wu, X.-F. Wan, Chem. Phys. Lett. 424 (2006) 387.
[39] A. Mallick, B. Haldar, N. Chattopadhyay, J. Phys.Chem. B 109 (2005) 14683.
[40] S. Panja, P. Chowdhury, S. Chakravorti, Chem. Phys. Lett. 393 (2004) 409.
[41] A. Bajorek, J. Paczkowski, Macromolecules 31 (1998) 86.
[42] J.A. Bautista, R.E. Connors, B.B. Raju, R.G. Hiller, F. P Sharples, D. Goszlota, M.R. Wasielewski, H.A. Frank, J. Phys. Chem. B 103 (1999) 8751.
[43] R.R. Rando, Chem. Rev. 101 (2001) 1881.
[44] W. Rettig, Angew. Chem. Int. Ed. Engl. 25 (1986) 971.
[45] T. Fournier, S. Pommeret, J-C. Mialocq, A. Deflandre, R. Rozot, Chem. Phys. Lett. 325 (2000) 171.
[46] D. Gormin, M. Kasha, Chem. Phys. Lett. 153 (1988) 574.
[47] P.-T. Chou, W.-S. Yu, Y.-M. Cheng, S.-C. Pu, Y.-C. Yu, Y.-C. Lin, C.-H. Haung, C.-T. Chen, J. Phys. Chem. A 108 (2004) 6487.
[48] S. Rios Vazquez, M.C. Rios Rodriguez, M. Mosquera, F. Rodriguez-Prieto, J. Phys. Chem. A 111 (2007) 1814.
[49] S. Rios Vazquez, M.C. Rios Rodriguez, M. Mosquera, F. Rodriguez-Prieto, J. Phys.Chem. A 112 (2008) 376.
[50] A.U. Acuna, J. Catalan, F. Toribio, J. Phys. Chem. 85 (1981) 241.
[51] J. Catalan, F. Toriblo, A.U. Acuna, J. Phys. Chem. 86 (1982) 303.
[52] S. Nagaoka, N. Hirota, M. Sumitani, K. Yoshihara, J. Am. Chem. Soc. 105 (1983) 4220.
[53] T. Nishiya, S. Yamauchi, N. Hirota, Y. Fujiwara, M. Itoh, J. Am. Chem. Soc. 108 (1986) 3880.
[54] T. Nishiya, S. Yamauchi, N. Hirota, M. Baba, I. Hanazaki, J. Phys. Chem. 90 (1986) 5730.
[55] S. Nagaoka, N. Hirota, M. Sumitani, K. Yoshihara, E. Lipczynska-Kochany, H. Iwamura, J. Am. Chem. Soc. 106 (1984) 6913.
[56] S. Nagaoka, U. Nagashima, N. Ohta, M. Fujita, T. Takemura, J. Phys. Chem. 92 (1998) 166.
[57] S. Dahne, W. Freyer, K. Teuchner, J. Dobkowski, Z.R. Grabowski, J. Lumines. 22 (1980) 37.
[58] W. Rettig, B. Zietz, Chem. Phys. Lett. 317 (2000) 187.
[59] C.C.J. Roothan, Rev. Mod. Phys. 23 (1951) 69.
[60] W. Khon, L.J. Sham, Phys. Rev. 140 (1965) A1133.
[61] P. Hohenberg, W. Kohn, Phys. Rev. B 136 (1964) 864.
[62] A.K. Shaw, S.K. Pal, J. Photochem. Photobiol. B 86 (2007) 99.
[63] Gaussian 03, Revision B.03, M.J. Frisch, et al., Gaussian, Inc., Pittsburgh PA, 2003.
[64] A. Dreuw, M. Head-Gordon, Chem. Rev 105 (2005) 4009.
[65] J.M. Ortiz-Sánchez, R. Gelabert, M. Moreno, J.M. Lluch, J. Phys. Chem. A 110 (2006) 4649.
[66] J. Neugerbauer, O. Gritsekbo, E. Jan Baerends, J. Chem. Phys. 124 (2006) 214102.
[67] C.J. Jamorski, H.P. Lüthi, J. Chem.Phys. 119 (2003) 12852.
[68] (a) H. Lampert, W. Mikenda, A. Karpfen, J. Phys. Chem. A 101 (1997) 2254;
(b) S.J. Grabowski, Annual Report C 102 (2006) 131.
[69] B.A. Zadorozhnyi, I.K. Ishchenko, Opt. Spectros. (Engl. Trans.) 19 (1965) 306.
[70] R.M. Badger, S.H. Bauer, J. Chem. Phys. 5 (1937) 839.